Boukley Hasan, W., Harris, P., Doufexi, A., & Beach, M. (2018). Spatial Uplink Power Control for Massive MIMO. In *2017 IEEE 85th Vehicular Technology Conference (VTC Spring): Proceedings of a meeting held 4-7 June 2017, Sydney, Australia.* (pp. 2541-2546). (VTS : Vehicular Technology Conference : VTC). Institute of Electrical and Electronics Engineers (IEEE). https://doi.org/10.1109/VTCSpring.2017.8108658

Peer reviewed version

License (if available):
Other

Link to published version (if available):
10.1109/VTCSpring.2017.8108658

Link to publication record in Explore Bristol Research
PDF-document

Spatial Uplink Power Control for Massive MIMO

Wael Boukley Hasan, Paul Harris, Angela Doufexi and Mark Beach
Communications Systems & Networks Group, University of Bristol, Bristol, BS8 1UB, UK
Email: {wb14488, paul.harris, a.doufexi, m.a.beach}@bristol.ac.uk

Abstract—**This paper proposes a novel uplink power control scheme in a single cell for massive MIMO (Multiple-Input-Multiple-Output). The proposed algorithm exploits the spatial degrees of freedom provided by massive MIMO to achieve the highest signal to interference-plus-noise ratio (SINR) for each user by considering the mutual spatial correlation arising from other users. It also minimizes the required uplink transmit power to achieve the highest possible uplink SINR per user without increasing the complexity at the user equipment. The base station (BS) controls the user transmit power using only two bits in a Transmission Power Control (TPC) command and the newly introduced algorithm is expected to increase both the energy efficiency (EE) and single cell spectral efficiency (SE) with reduced transmission overhead, latency and complexity in the receiver. Through recent preliminary trials, a 0.9 dB average SINR increase was achieved, and transmit power was decreased by up to 2.5 dB in the uplink. The proposed algorithm supports several popular linear MIMO decoders and precoders including Minimum Mean Square Error (MMSE), Zero-Forcing (ZF) and Matched Filtering (MF).**

Keywords — Massive MIMO, Power Control, Field Trail, 5G.

I. Introduction

Massive multiple-input-multiple-output (MIMO) has recently become a strong candidate for 5G. The unprecedented per-cell bandwidth efficiency of 146.5 bit/s/Hz achieved in [1, 2] supports the trend towards using this technology in 5G. Massive MIMO is a Multi-User (MU)-MIMO system with a large number of antennas at the Base station (BS) serving several users within the same time and frequency resource [3]. The large number of antennas at the BS has a great impact on the system's performance. Many potential advantages are expected and numerous implementation challenges are addressed in [11]. Theoretically, the spectrum efficiency (SE) and the energy efficiency (EE) should be increased [12], and in [1], the improvement in SE has been demonstrated. In addition, the 'channel hardening' synonymous with massive MIMO technology [9] was also observed in these field experiments and this phenomenon could be exploited to increase the link EE if uplink (UL) power control is considered.

In Long-Term Evolution (LTE), open loop and closed loop algorithms are used for power and signaling control. The minimum signaling rate depends on operational conditions (environment and dynamics). The open loop algorithm is used when the user equipment (UE) joins the system or when the channel conditions vary, while the closed loop algorithm is used when the channel conditions are more stable. In the open loop mode, the UE derives the desired UL power level by importing different values, sent from the BS, into a predetermined equation [7]. While in the closed loop mode, the UE adjusts the UL power according to the transmission power control (TPC) command sent by the BS. The TPC command is interpreted according to a predetermined lookup table which increases or decreases the UL power level with constant values [14].

A simple receiver with a basic UL power control design is desirable for massive MIMO [10], yet little research has been conducted on this topic. The UL power control algorithm in [4] is based on a minimum mean-square-error (MMSE) receiver, which brings with it significant complexity.

The UL power control presented here has two stages: the average UL signal to interference-plus-noise ratio (SINR) is determined, which is considered as the lower bound, followed by a joint iterative pilot and data power control algorithm. The work in [5] has considered power control for a single cell. It maximizes the minimum SE by converting it into a geometric program (GP) and finds the local maximum points. A joint power and data allocation algorithm is proposed in [6] which tends to improve the uplink EE based MMSE channel estimation followed by maximum ratio combining (MRC) receive processing. The UL power control algorithms proposed so far for massive MIMO are based on pilot and data power allocations amongst users, either within the same or adjacent cells. To the best of the author's knowledge, no power control technique designed for massive MIMO has yet been tested in a field trial.

In this paper, we propose a simple closed loop UL power control algorithm based only upon the pilot channel estimation. Simple open loop UL power control is still needed prior to the proposed closed loop UL power control. We believe that the channel hardening phenomenon in massive MIMO provides an improved channel robustness which allows for fewer UL power control adjustments [19,20]. A novel TPC mapping and de-mapping algorithm is proposed to obtain a high EE by transmitting only the minimum power required. Furthermore,

978-1-5090-5932-4/17/$31.00 ©2017 IEEE

the single cell SE is increased by decreasing the spatial correlation between UEs.

II. System Model

A single-cell Massive-MIMO architecture is considered in this work. The base station (BS) is equipped with M antennas and serves K single-antenna users simultaneously where (M >> K). The system operates in Time-division Duplex (TDD) mode and uses the same time-frequency resources for all users. The user equipment (UE) transmits an UL pilot with power **P** for the channel estimation.

The channel matrix between the UEs and the BS is denoted by $\mathbf{H} \in \mathbb{C}^{M \times K}$. The channel matrix, frame schedule and MIMO processing are explained in [18]. The BS derives the user-side Gram matrix **W**, which is given by:

$$\mathbf{W} = \mathbf{H}^{\mathbf{H}}\,\mathbf{H} \tag{1}$$

It then approximates the SINR for each UE using the correlation results provided by the Gram matrix and saves the values for a short time window. All mentions of SINR or inter-user interference from here forward refer to this correlation based approximation. The maximum and minimum accepted SINR are predetermined and saved at the BS as a threshold based on the modulation and coding scheme (MCS) in use. For the field trial described in section IV, the maximum SINR threshold ($\mathrm{SIRN_{max}}$) is the lowest SINR value required for a sufficient transmission by using 256-QAM. Similarly, the minimum SINR threshold ($\mathrm{SIRN_{min}}$) is the lowest SINR value required for a sufficient transmission using BPSK based access.

The large number of antennas at the BS affects the MIMO channel by causing a very slow growth in the variance of mutual information compared to its mean. As a result, the off-diagonal values of the **W** matrix become increasingly weaker compared to the diagonal value. This phenomenon is called channel hardening and becomes more prominent as the number of antennas is increased. .

III. Uplink Power Control Algorithm

The proposed algorithm exploits the improved channel robustness and hardening that results from using a large number of antennas at the BS. It is based only on the physical layer parameters. The BS determines the transmit power level for each UE in the system. It controls the power level adjustment and sends it to the UEs by using a TPC command. A simple UL open loop power control is needed prior applying the adjustment mechanism.

The BS has an acceptable inter-user spatial correlation threshold ($\mathrm{I_{Th}}$) which represents the acceptable ratio between $\mathrm{w_{ii}}$ and $\mathrm{w_{ij}}$. The UEs with high spatial correlation are paired according to the following equation:

$$\mathbf{CU}_{\mathrm{n}} = \{\mathbf{UE}_{\mathrm{i}}\,, \mathbf{UE}_{\mathrm{j}}\} \tag{2}$$
$$\text{subject to } \mathrm{w_{ij}} > \mathrm{I_{Th}} \qquad ,i \neq j$$
$$\text{where } \mathrm{i,j} \in [1,\mathrm{K}], \mathrm{n} \in [1, \mathrm{K}-1]$$

CU denotes the correlated users. The BS then approximates the SINR range for each pair as follows:

$$\mathrm{SINR\ Range_n} = \left|\mathrm{SINR_i} - \mathrm{SINR_j}\right| \tag{3}$$

The adjustment mechanism at the BS divides the UEs into three groups based on SINR and $\mathrm{I_{Th}}$ values. Each group targets a desired SINR value (DSINR). The groups are illustrated in figure 1, and are divided as follows:

1. Group 1: (red arrows) The UE SINR value $\notin$ [$\mathrm{SINR_{min}}$, $\mathrm{SINR_{max}}$]. The BS tells the UE to increase or decrease its power so that the received SINR reaches the acceptable range.

2. Group 2: (green arrows) The UE SINR is within the acceptable range and the SINR Range value is > 0.5 dB (in this work, a 0.5dB step-size has been adopted as the minimum resolution). The BS assigns a desirable SINR for both UEs as follows:

   $$\mathrm{DSINR_n} = \min(\mathrm{SINR_n}) \tag{4}$$

   The BS then tells each UE to change its transmit power so that the received SINR for both users = DSINR ± 0.5dB.

3. Group 3: (blue arrows) Either the UEs have low spatial correlation or the SINR Range is less than 0.5dB. In both cases, the BS will tell the UEs to increase their transmit power if it doesn't reach the maximum threshold or it will tell them to keep using the same transmit power.

The SINR values in group 2 are adjusted into DSINR. This is going to reduce the spatial correlation between the UEs. In group 3 the spatial correlation will already be low, so the BS starts to increase the SINR for both UEs by increasing their transmitting power. This step will ensure that the SINR growth for the UEs won't affect the others, and thus, the BS ensures the SINR converges between the correlated UEs into the maximum harmless level between them, where any additional increment would affect other UEs. The UEs in our design do not estimate the SINR or the distance; they only apply the power adjustment according to the received TPC command. This will reduce the complexity of the receiver as well as the overheads sent by the BS. Open loop power control is still required when the users join the system, but can then be followed by the proposed UL power control in this paper.

IV. Supporting Experiments

The proposed UL power control algorithm is based upon the assumption that massive MIMO technology achieves highly improved channel robustness. Three different experiments have been performed so far. The first one, explained in sections A and B, aims to investigate the practicality of implementing the proposed algorithm. Real time channel measurements were taken by the massive MIMO testbed described in [13]. Twelve single antenna clients from 6 USRPs (Universal Software Radio Peripherals) were supported simultaneously at a 3.51 GHz carrier frequency sharing a common 20MHz radio channel. On the second experiment, the proposed PC algorithm was implemented on the massive MIMO testbed [16], which is illustrated in section C. For testing purposes, the TPC update rate was set to 2 times per second in the second experiment. In the third experiment, the TPC update rate was increased to 10 times per second.

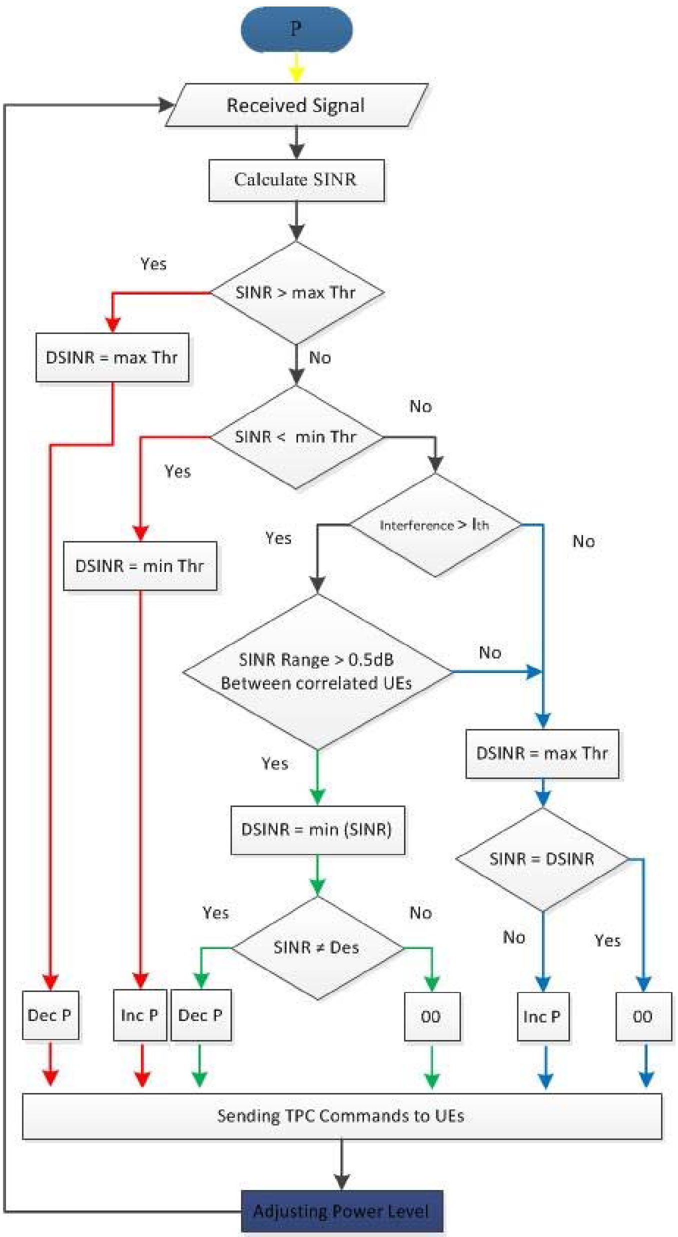

Fig. 1. Spatial uplink power control algorithm for massive MIMO. Red arrows are group 1. Green arrows are group 2. Blue arrows are group 3. Shapes filled in blue are at the UE while others are at the BS.

A. MU-MIMO Channel Robustness with 32 Antennas

The MU-MIMO channel was initially measured indoors by the massive MIMO testbed with 32 active BS antennas. The distance between the BS and the 12 single antenna clients was 20.81m and a static environment was maintained. Figure 2, showing the **W** matrix, is obtained from equation 1 for the real valued channel model. The figure was averaged over 100 captures of the channel measurement data.

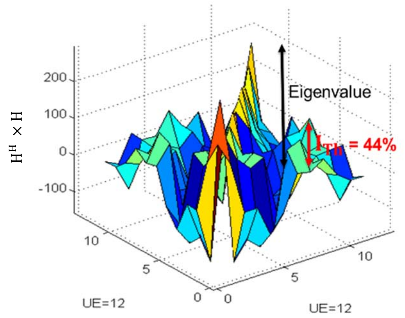

Fig. 2. $\mathbf{H}^H \times \mathbf{H}$ Channel Gram Matrix for MU-MIMO. 32 antennas at the BS and 12 UEs, where Each UE has 1 antenna (not normalized).

B. Massive-MIMO Improved Channel Robustness

Here, the channel was measured by the massive MIMO testbed with 112 active antennas at the BS. The distance between the BS and the 12 single antenna clients was 11.6 m. Three people walked pseudo-randomly during the channel measurements. One person walked right next to the client antennas, while the others were walking between the BS and the clients. The client transmit power was adjusted before the channel measurements, but power control was not used during this set of measurements. Figure 3 illustrates the greatly improved channel robustness averaged over 400 captures of the channel measurement data, and the channel hardening phenomenon can be clearly seen. . These conditions would allow our proposed algorithm to work effectively. By comparing the results from Figure 2 and Figure 3, the ratio between w_{ii} and the max w_{ij} was decreased from 44% to 16%. Therefore, less UEs require the paring process in equation 2, which means less UEs are considered in group 2. Most of the UEs will be assigned into group 3 which only requires an increment on the UE transmit power till it reaches the $SINR_{max}$. Once $w_{ij} > I_{Th}$ occurs (where $i \neq j$), the UEs will be assigned into group 2, which reduces the spatial correlation between them. This process allows the UEs to achieve the highest possible SINR with the minimum transmit power. If the proposed algorithm is used for the case of 32 antenna MU-MIMO, the SINR convergence process in group 2 requires more time and may not converge due to the channel conditions.

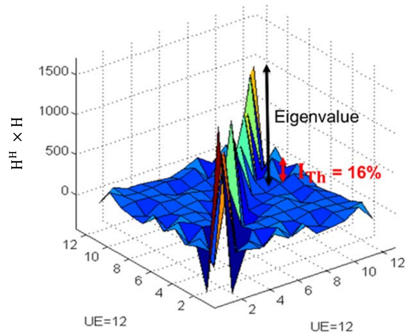

Fig. 3. $\mathbf{H}^H \times \mathbf{H}$ Channel Gram Matrix for Massive MIMO. 112 antennas at the BS and 12 UEs, where UE each has 1 antenna (not normalized).

C. *Massive MIMO with Power Control (Indoor Trial)*

A Massive MIMO power control algorithm was designed based on the results we obtained from the first experiment [15] and subsequently implemented on the BIO massive MIMO testbed. The clients were divided into three groups with different distances as shown in Figures 4 and 5. Each group has 4 UEs, as shown in Figure 6, and the BS has a 128 element patch antenna array.

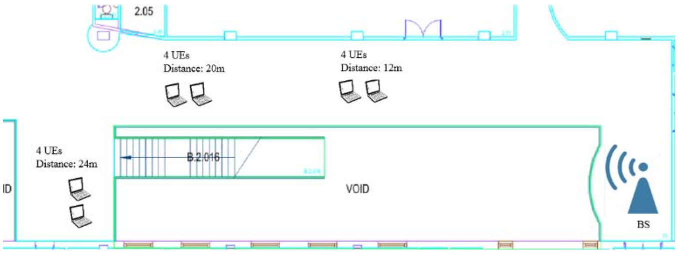

Fig. 4. UE Distribution within the indoor atrium measurements at Merchant Venturers Building (floor-plan).

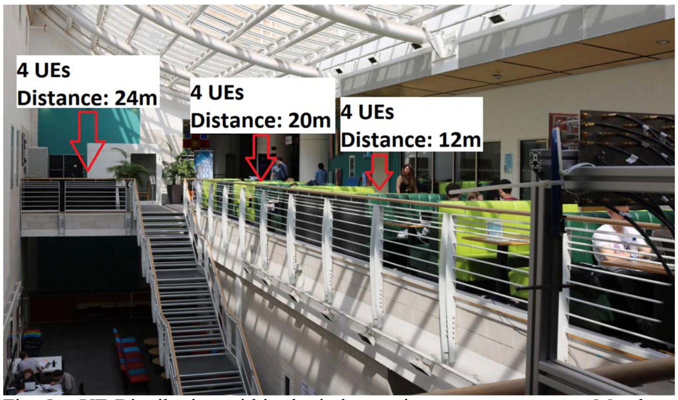

Fig. 5. UE Distribution within the indoor atrium measurements at Merchant Venturers Building.

Fig. 6. Number of UEs in one group. Each laptop and USRP represents two UEs with a single antenna. The total number of UEs is four.

The environment was changing during channel measurements, although the client devices remained static, and three different PC algorithms were tested. The first and the second PC algorithms are based on a fixed SNR\SINR value, where the BS adjusts the UEs power level to a certain SNR\SINR value. The third PC is the one proposed on this paper to maximize the SINR per user and the overall SINR. 800 captures of the channel measurement data were taken. The channel conditions when the fixed SNR PC algorithm was used are illustrated in Figure 7.

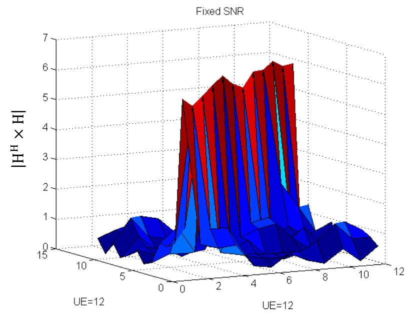

Fig. 7. Plot $|\mathbf{H}^{H} \times \mathbf{H}|$ for Massive MIMO where the fixed SNR PC algorithm was used. 128 antennas at the BS and 12 UEs, where each has 1 antenna for the user locations shown in Figure 5.

Although the TPC update rate is only 2 times per second, the channel conditions are stable since the ratio between the w_{ii} and w_{ij} is below 20% (where $i \neq j$). When the proposed PC algorithm was implemented, the UEs increased their power level. The power increment was controlled by the spatial correlation threshold as explained in section A in the adjustment mechanism. Figure 8 shows the channel conditions associated with the proposed PC algorithm.

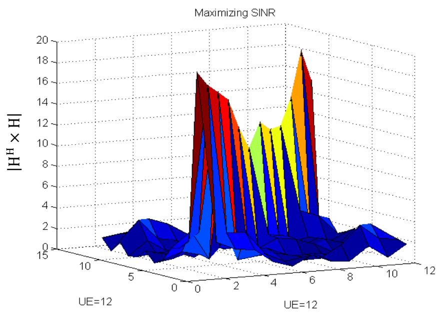

Fig. 8. Plot $|\mathbf{H}^{H} \times \mathbf{H}|$ for Massive MIMO where the proposed PC algorithm was used. 128 antennas at the BS and 12 UEs, where each has 1 antenna for the user locations shown in Figure 5.

The results obtained from the experiment are illustrated in Table I and in Figure 9. The average SINR per user and the overall average SINR were measured based on the three different PC algorithms. When the BS adjusts the UEs power level to a fixed SNR value, the aggregate average SINR for all the UEs was 5.4 dB. This value was increased by 0.4 dB when the adjustment was based on the SINR. The maximum SINR was achieved when the UEs' power adjustments were based on the proposed PC algorithm. It enhanced the total average SINR by 0.5 dB compared to when a fixed SINR was used. At present, the power control adjustments are made with a 0.5 second update rate; thus, the UE may increase the power above the accepted limit (where it starts to cause high spatial correlation) if there is significant motion in our indoor environment. With a higher TPC update rate, the performance will be enhanced, since the UEs will reduce their transmit power once they reach the spatial correlation threshold and will not have to wait 0.5 seconds for the next TPC command. Clearly, this will reduce the spatial correlation and increase the SINR.

Table I. Aggregate average SINR based on three different PC algorithms

	Aggregate Average SINR (dB)
PC with fixed SNR	5.4
PC with fixed SINR	5.8
Spatial UL PC for M-MIMO	6.3

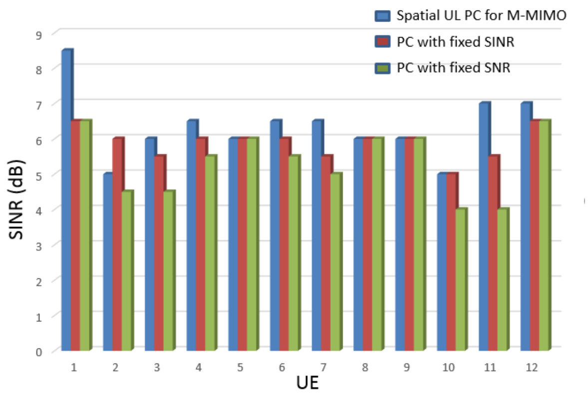

Fig. 9. The average SINR per user based on three different PC algorithms (Indoor Trial)

D. Massive MIMO with Power Control (Outdoor Trial)

Following the previous trials, an outdoor experiment took place in the University of Bristol's Merchant Venturers Building Courtyard. Two scenarios were measured in this trial. In the first scenario, 6 USRPs were divided into three groups and the BS has a 128-element patch antenna array as shown in Figure 10. Only one UE was active from each USRP. In the second scenario, the 6 USRPs were reallocated to group 2 and two UEs were active from each USRP.

Fig. 10. Panoramic view of massive MIMO outdoor trial set-up (Merchant Venturers Building Courtyard)

Two different UL PC algorithms were tested in this experiment for both scenarios. The first is the one proposed in this paper, whilst the second is based on a fixed SNR value (where the BS adjusts the UEs power level to a certain SNR value). The average SINR values per user are illustrated in Figure 11 for the first scenario and in Figure 13 for the second scenario. In the first scenario, the aggregate average SINR for all the users achieved by the proposed spatial UL PC algorithm was 12.5 dB and the aggregate average SNR was 14 dB as it is shown in Table II. With a 13 dB SNR UL PC, the aggregate average SINR was 11.6 dB and the aggregate average SNR was 13 dB. Since the aggregate average SNR value from the proposed spatial UL PC was larger than the one obtained from the PC with 13 dB fixed SNR, the SNR reference value was increased to 16.5 dB which increased the aggregate average SNR by 3.5 dB and the aggregate average SINR by 0.9 dB. The average SNRs per user are illustrated in Figure 12. Since the UEs remained static during the three measurements, the path loss should be the same. Which means the proposed spatial UL PC algorithm decreased the required UL power level by 2.5 dB to achieve an aggregate average SINR of 12.5 dB.

Table II. Aggregate average SINR and SNR based on three different UL power control techniques

	Aggregate Average SINR (1st Scenario)	Aggregate Average SNR (1st Scenario)	Aggregate Average SINR (2nd Scenario)
Spatial UL PC	12.5 dB	14 dB	5.6 dB
PC with fixed SINR (1st Scenario 13 dB, 2nd Scenario 11.5 dB)	11.6 dB	13 dB	5 dB
PC with fixed SINR (1st Scenario 16 dB, 2nd Scenario 15.5 dB)	12.5 dB	16.5 dB	4.8 dB

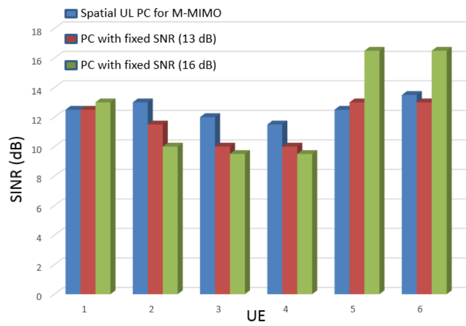

Fig. 11. The average SINR per user based on three different PC algorithms (The 1st scenario of the outdoor trial)

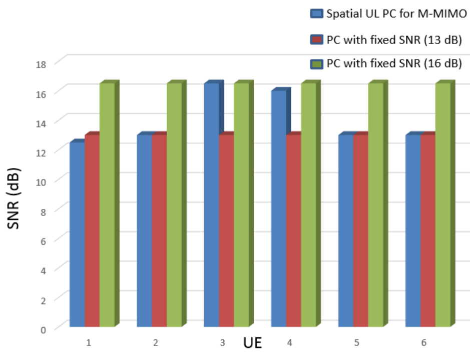

Fig. 12. The average SNR per user based on three different PC algorithms (The 1st scenario of the outdoor trial)

In the second scenario, the aggregate average SINR for the twelve UEs was 5.6 dB when the proposed spatial UL PC was used. This value was decreased by 0.6 dB when the UL power level adjustment was based on an SNR reference level of 11.5 dB. The SNR reference level was then increased to 15.5 dB to increase the average SINR. Although the adjustment level was increased by 4 dB, the aggregate average SINR was decreased by 0.2 dB. The reason behind this decrement is the interference added to each user from the other eleven users. The separation distance between the USRPs in the second scenario is small compared to the first one, which led to higher spatial correlation between the 12 UEs. That is, increasing the UL power level might lead to a point where the increment of the aggregate inter-user spatial correlation from all the users would be more than the increment for the received signal power.

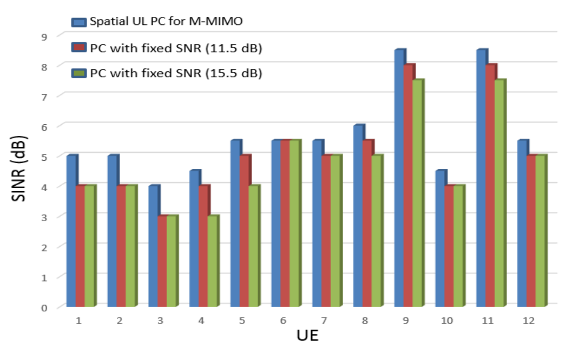

Fig. 13. The average SINR per user based on three different PC algorithms (The 2nd scenario of the outdoor trial)

V. CONCLUSION

This paper has proposed a spatial UL power control algorithm for massive MIMO which can increase both the EE and the single cell SE. Only a small overhead is required to adjust the transmit power level at the UEs since only two bits are required for the TPC. By carefully considering the spatial correlation levels provided by the user-side Gram matrix, a maximum SINR can be safely achieved for each UE in the system. With the proposed algorithm, the average SINR was increased for most of the UEs, with an aggregate average SINR increment of up to 0.9 dB and an aggregate average UL power decrement of up to 2.5 dB. In ongoing work, the effects of user mobility on massive MIMO will be considered to determine how much the PC update rate could be reduced for such a systemwhilst still maintaining an acceptable level of performance.

ACKNOWLEDGMENT

The authors wish to thank Bristol is Open [17] for access to the hardware facility and the financial support from the EPSRC (CDT in Communications, EP/I028153/1) and BBC R&D. Contributions from the University of Lund (Professors Edfors and Tufvesson and their team) alongside that from National Instruments (Nikhil Kundargi and Karl Nieman) in the on-going development of the Massive MIMO Reference Design are most gratefully acknowledged.

REFERENCES

[1] University of Bristol [online]. Availalable: http:// http://goo.gl/ZOj5kr.

[2] IEEE Spectrum [online]. Availalable: http:// goo.gl/5Dlqjv.

[3] T. L. Marzetta, "Noncooperative cellular wireless with unlimited numbers of base station antennas," IEEE Trans. Wireless Commun., vol. 9, no. 11, pp. 3590–3600, 2010.

[4] K. Guo, Y. Guo, G. Fodor and G. Ascheid, "Uplink power control with MMSE receiver in multi-cell MU-massive-MIMO systems," ICC, Sydney, NSW, 2014, pp. 5184-5190.

[5] Hei Victor Cheng. Emil Bj¨ornson, Erik G.Larsson, "Uplink Pilot and Data Power Control for Single Cell Massive MIMO Systems with MRC," arXiv:1509.02633v1, Sep. 2015.

[6] K. Guo, Y. Guo and G. Ascheid, "Energy-Efficient Uplink Power Allocation in Multi-Cell MU-Massive-MIMO Systems," European Wireless 2015; 21th European Wireless Conference; Proceedings of, Budapest, Hungary, 2015, pp. 1-5.

[7] Sonia, Nisha Malik, Preet Kanwar Singh Rekhi and Sukhvinder Singh Malik, "Uplink Power Control Schemes in Long Term Evolution," Volume-3, Issue-3, IJEAT, February 2014, ISSN: 2249 – 8958.

[8] Zarrinkoub, Houman, "Link Adaptation" in Understanding LTE With MATLAB, 1st ed, Chichester, England: John Wiley & Sons, Ltd, 2014.

[9] T. L. Narasimhan and A. Chockalingam, "Channel Hardening-Exploiting Message Passing (CHEMP) Receiver in Large-Scale MIMO Systems," in IEEE Journal of Selected Topics in Signal Processing, vol. 8, no. 5, pp. 847-860, Oct. 2014.

[10] L. Wang; H. Q. Ngo; M. Elkashlan; T. Q. Duong; K. K. Wong, "Massive MIMO in Spectrum Sharing Networks: Achievable Rate and Power Efficiency," in IEEE Systems Journal , vol.PP, no.99, pp.1-12.

[11] L. Lu, G. Y. Li, A. L. Swindlehurst, A. Ashikhmin and R. Zhang, "An Overview of Massive MIMO: Benefits and Challenges," in IEEE Journal of Selected Topics in Signal Processing, vol. 8, no. 5, pp. 742-758.

[12] Xin Fang, Y. Zhang, Haiyan Cao and Na Ying, "Spectral and energy efficiency analysis with massive MIMO systems," 2015 IEEE 16th ICCT, Hangzhou, 2015, pp. 837-843.

[13] P. Harris, S. Zang, A. Nix, M. Beach, S. Armour and A. Doufexi, "A Distributed Massive MIMO Testbed to Assess Real-World Performance and Feasibility," VTC Spring, 2015 IEEE 81st, Glasgow, 2015, pp. 1-2.

[14] "LTE; evolved universal terrestrial radio access (E-UTRA); physical layer procedures," ETSI TS 136 213 V8.8.0 (2009-10).

[15] University of Bristol [online]. Availalable: http:// goo.gl/SNrNvw.

[16] Paul Harris etc, "LOS Throughput Measurements in Real-Time with a 128 Antenna Massive MIMO Testbed", EURO-COST, TD (16)01085, Lille.

[17] Bristol is Open [online]. Available: http://www.bristolisopen.com/.

[18] P. Harris et al., "Serving 22 Users in Real-Time with a 128-Antenna Massive MIMO Testbed," 2016 IEEE International Workshop on Signal Processing Systems (SiPS), Dallas, TX, USA, 2016, pp. 266-272.

[19] P. Harris,S. Malkowsky, J. Vieira et al., "Performance Characterization of a Real-TimeMassive MIMO System with LOS Mobile Channels," IEEE JSAC Deployment Issues and Performance Challenges for 5G, submitted, 2016.

[20] P. Harris,S. Malkowsky, J. Vieira et al., "Temporal Analysis of Measured LOS Massive MIMO Channels with Mobility," IEEE VTC Recent Results in 5G Innovation, submitted, 2017.